



Ocean acidification mediates photosynthetic response to UV radiation and temperature increase in the diatom *Phaeodactylum tricornutum*

Y. Li¹, K. Gao¹, V. E. Villafañe², and E. W. Helbling²

¹State Key Laboratory of Marine Environmental Science, Xiamen University, Xiamen, 361005, China

²Estación de Fotobiología Playa Unión and Consejo Nacional de Investigaciones Científicas y Técnicas (CONICET) Casilla de Correos No. 15 (9103) Rawson, Chubut, Argentina

Correspondence to: K. Gao (ksgao@xmu.edu.cn)

Received: 1 June 2012 – Published in Biogeosciences Discuss.: 18 June 2012

Revised: 11 September 2012 – Accepted: 13 September 2012 – Published: 12 October 2012

Abstract. Increasing atmospheric CO₂ concentration is responsible for progressive ocean acidification, ocean warming as well as decreased thickness of upper mixing layer (UML), thus exposing phytoplankton cells not only to lower pH and higher temperatures but also to higher levels of solar UV radiation. In order to evaluate the combined effects of ocean acidification, UV radiation and temperature, we used the diatom *Phaeodactylum tricornutum* as a model organism and examined its physiological performance after grown under two CO₂ concentrations (390 and 1000 μatm) for more than 20 generations. Compared to the ambient CO₂ level (390 μatm), growth at the elevated CO₂ concentration increased non-photochemical quenching (NPQ) of cells and partially counteracted the harm to PS II (photosystem II) caused by UV-A and UV-B. Such an effect was less pronounced under increased temperature levels. The ratio of repair to UV-B induced damage decreased with increased NPQ, reflecting induction of NPQ when repair dropped behind the damage, and it was higher under the ocean acidification condition, showing that the increased pCO₂ and lowered pH counteracted UV-B induced harm. As for photosynthetic carbon fixation rate which increased with increasing temperature from 15 to 25 °C, the elevated CO₂ and temperature levels synergistically interacted to reduce the inhibition caused by UV-B and thus increase the carbon fixation.

1 Introduction

The increase in atmospheric CO₂ concentration is expected to influence the acid–base balance in the pelagic (McNeil and Matear, 2008) as well as in the coastal waters (Cai et al., 2011) due to increasingly dissolved CO₂, leading to ocean acidification (Sabine et al., 2004). By the end of this century, atmospheric CO₂ levels are expected to increase to 800–1000 ppmv (IPCC A1F1 scenario), while surface seawater pH would be reduced by 0.3–0.4 pH units (100–150 % increase in H⁺ concentration) (Caldeira and Wickett, 2003; Orr et al., 2005). Ocean acidification is known to reduce calcification of coccolithophores (Beaufort et al., 2011; Riebesell and Tortell, 2011) and coralline algae (Gao et al., 1993; Gao and Zheng, 2010). On the one hand, increasing pCO₂ in seawater has been shown to stimulate growth and photosynthetic carbon fixation rates of phytoplankton (Hein and Sand-Jensen, 1997; Schippers et al., 2004; Riebesell et al., 2007; Wu et al., 2010; McCarthy et al., 2012), while neutral effects of CO₂ enrichment were also reported (Tortell et al., 2000; Tortell and Morel, 2002; Fu et al., 2007). On the other hand, the increase in pCO₂ may alter phytoplankton community structure (Tortell et al., 2002), and enhance mitochondria respiration (Wu et al., 2010). Ocean acidification is not an isolated process, and thus interactive effects with other climate changes, like increasing temperature and UV radiation (UVR, 280–400 nm), need to be considered in an holistic way (Boyd, 2011; Hutchins, 2011).

With increasing atmospheric CO₂ concentration, global temperature is expected to increase by 2.5–6.4 °C in the

atmosphere (Alexiadis, 2007) and by 2–3 °C in the surface oceans by the year 2100 (Houghton et al., 2001). Such changes will also have important effects on various organisms, since most physiological processes are temperature-dependent (Allakhverdiev et al., 2008). It is known that temperature affects the morphology (Mühling et al., 2003) and biochemical composition (Mühling et al., 2005) of cyanobacteria. However, differential responses to the combined “greenhouse” (warming as well as elevated CO₂) treatment have been found in the marine picocyanobacteria *Synechococcus* and *Prochlorococcus*, with the growth rate of the former increasing and that of the latter not changing (Fu et al., 2007). Hutchins et al. (2007) reported that either elevated CO₂ (750 ppmv) or a 4 °C temperature increase stimulated the growth and nitrogen fixation rate of the filamentous cyanobacterium *Trichodesmium* sp., however synergistic effects among these two variables had not been observed. A 5 °C temperature rise only increased photosynthesis and calcification of *Emiliania huxleyi* grown under Ca²⁺ sufficient but not under Ca²⁺ deficient conditions (Xu et al., 2011). Nevertheless, the “greenhouse” increased the coccolithophore cell abundance (Feng et al., 2009). The distributions and ecological niches of major phytoplankton groups like dinoflagellates (Peperzak, 2003; Cloern et al., 2005; Hallegraeff, 2010), diatoms, and coccolithophores (Merico et al., 2004; Hare et al., 2007) have been suggested to change with ocean warming. The acceleration of the spring phytoplankton bloom and changes in dominant species were affected by the combination of warming and high light levels (Lewandowska and Sommer, 2010). It is known that a “stratified greenhouse” of the surface oceans has been affected by progressive oceanic warming and acidification (Doney, 2006; Beardall et al., 2009), therefore, phytoplankton cells will be exposed to “greenhouse” under increasing exposures to solar visible and ultraviolet radiation (UVR, 280–400 nm).

Solar UV-B (280–315 nm) radiation at the Earth’s surface has been shown to increase due to the ozone depletion and its interplay with climate change (Manney et al., 2011). UVR (UV-A + UV-B) is known to inhibit growth and photosynthesis (Helbling et al., 1992; Heraud and Beardall, 2000; Gao et al., 2007a; Jiang and Qiu, 2011) and damage proteins and the DNA molecule (Grzymalski et al., 2001; Xiong, 2001; Gao et al., 2008). However, moderate UVR levels were shown to increase photosynthetic carbon fixation (Nilawati et al., 1997; Barbieri et al., 2002), with UV-A (320–400 nm) even driving photosynthetic carbon fixation in the absence of PAR (Gao et al., 2007b).

In an ecological context, where organisms are exposed to the influence of several abiotic and biotic factors, the effects of multiple factors can greatly differ from simple combinations of single-factor responses (Christensen et al., 2006), that is, variables can act in synergistic or antagonistic ways (Dunne, 2010). For example, at ambient CO₂ level, the presence of UVR stimulated calcification of *E. huxleyi* (Guan and Gao, 2010), however at elevated CO₂ levels, it inhibited

calcification (Gao et al., 2009). Fu et al. (2008) reported that only simultaneous increases in both CO₂ and temperature enhanced the maximum light-saturated carbon fixation rate (P_{\max}^B) of the raphidophyte *Heterosigma akashiwo*, whereas CO₂ enrichment with or without increased temperature increased or reduced P_{\max}^B under high CO₂ or high temperature treatment, respectively, of the dinoflagellate *Prorocentrum minimum*. Under ocean acidification conditions, UV-B inhibited growth of the red tide alga *Phaeocystis globosa* (Chen and Gao, 2011).

Obviously, more attention is being paid to the study of the interactive effects of multiple stressors and ocean acidification on different taxonomic groups; however, diatoms have surprisingly received less attention. Changes in the seawater carbonate system, such as increased $p\text{CO}_2$ and HCO_3^- concentrations and decreased pH, may affect the phytoplankton energetics maintaining their intracellular acid–base stability, and thus their physiology coping with additional environmental changes. Consequently, we hypothesize that diatoms grown under ocean acidification conditions (high CO₂/lower pH) will be more sensitive to increases of UVR and temperature than cells grown at ambient CO₂ level. To test this hypothesis, we chose the cosmopolitan diatom species *Phaeodactylum tricorutum* as model organism, and the process studied was photosynthesis, via carbon incorporation and photochemical measurements.

2 Materials and methods

2.1 Organism model and culture conditions

Phaeodactylum tricorutum Bohlin (strain CCMA 106, isolated from the South China Sea (SCS) in 2004) was obtained from the Center for Collections of Marine Bacteria and Phytoplankton (CCMBP) of the State Key Laboratory of Marine Environmental Science, Xiamen University. Cultures were grown in 0.22 μm filtered natural seawater collected from the South China Sea (SEATS station: 116° E, 18° N) and enriched with Aquil medium (Morel et al., 1979). The cultures were maintained at 20 °C for about 20 generations before used in experiments. During this period, cultures were illuminated with cool white fluorescent tubes that provided 70 μmol photons m⁻² s⁻¹ of Photosynthetic Active Radiation (PAR; 12L:12D). The cultures (triplicate per each CO₂ condition) were continuously aerated (350 ml min⁻¹) with ambient CO₂ level (LC, 390 μatm) or CO₂ enriched (HC, 1000 μatm) air which was controlled with a CO₂ plant chamber (HP1000G-D, Wuhan Ruihua Instrument and Equipment Co., Ltd., Wuhan, China) with variations < 4 %.

Semi-continuous cultures were operated by diluting them with the CO₂-equilibrated media every 24 h, and the concentration of cells was maintained within a range of 7×10^4 – 3×10^5 cells ml⁻¹, so that the seawater carbonate system parameters were stable (Table 1) with pH variations < 0.02 units.

Table 1. Mean (\pm SD, $n = 24$) values of parameters of the seawater carbonate system under LC (ambient, 390 μ atm CO₂) and HC (enriched, 1000 μ atm CO₂) during the eight days prior to experiments. The superscripts represent significant difference between LC and HC.

$p\text{CO}_2$	pH_{NBS}	DIC ($\mu\text{mol kg}^{-1}$)	HCO_3^- ($\mu\text{mol kg}^{-1}$)	CO_3^{2-} ($\mu\text{mol kg}^{-1}$)	CO ₂ ($\mu\text{mol kg}^{-1}$)	Total alkalinity ($\mu\text{mol kg}^{-1}$)
LC	8.16 ± 0.01^a	1903.3 ± 47.66^a	1709.3 ± 39.2^a	181.2 ± 8.4^a	12.6^a	2171.0 ± 57.8^a
HC	7.82 ± 0.02^b	2127.3 ± 75.3^b	1998.3 ± 69.2^b	96.7 ± 6.7^b	32.3^b	2246.4 ± 84.0^a

The concentrations of cells were determined using a Coulter Counter (Z-2, Beckman) before and after the dilution (prior to the start of dark period). pH was measured with a pH meter (Benchtop pH 510, OAKTON) that was calibrated daily with a standard National Bureau of Standards (NBS) buffer (Hanna). Other parameters of the seawater carbonate system (Table 1) were calculated using the CO2SYS software (Lewis and Wallace, 1998) taking into account the salinity, $p\text{CO}_2$, pH, nutrient concentrations and temperature. The equilibrium constants K_1 and K_2 for carbonic acid dissociation and K_B for boric acid were determined according to Roy et al. (1993) and Dickson (1990), respectively.

2.2 Experimental setup

Samples of *P. tricornutum* (either from LC or HC, triplicate cultures for each CO₂ level) were harvested (concentration of $\sim 2 \times 10^5$ cells ml⁻¹), resuspended in fresh medium to a final concentration of $\sim 2 \times 10^4$ cells ml⁻¹ and put either in 35 or 100 ml quartz tubes (for carbon uptake or measurements of fluorescence parameters, respectively, see below). Three radiation treatments were implemented (with triplicate samples for each treatment): (1) PAB (PAR + UV-A + UV-B) treatment – quartz tubes covered with Ultraphan film 295 (Digefra, Munich, Germany), thus receiving irradiances above 295 nm; (2) PA (PAR + UV-A) treatment – quartz tubes covered with Folex 320 film (Montagefolie, Folex, Dreieich, Germany), samples receiving irradiances above 320 nm; and (3) P treatment – quartz tubes covered with Ultraphan film 395 (UV Opak, Digefra), samples receiving only PAR (400–700 nm). The transmission of these cut-off foils and quartz tubes are available elsewhere (Figueroa et al., 1997). The tubes for carbon incorporation and for fluorescence measurements were placed under a solar simulator (Sol 1200 W; Dr. Hönle, Martinsried, Germany). The cells were exposed to irradiances of 63.5 W m⁻² (PAR, 290 $\mu\text{mol photons m}^{-2} \text{s}^{-1}$), 23.1 W m⁻² (UV-A) and 1.20 W m⁻² (UV-B) for 60 min under three temperature levels: 15, 20 and 25 °C, by maintaining the tubes in a circulating water bath for temperature control (CTP-3000, Eyela). During the exposures, measurements of fluorescence parameters were done (see below); after exposure, part of the samples were processed for carbon uptake measurements, while part of them were allowed to recover for 80 min (under the initial growth light level of 70 $\mu\text{mol photons m}^{-2} \text{s}^{-1}$), dur-

ing which fluorescence parameters were measured (see below).

2.3 Measurements and analysis

2.3.1 Radiation measurements

The irradiances received by the cells were measured using a cosine response broad-band filter radiometer (ELDONET, Real Time Computer, Möhrendorf, Germany) that has channels for UV-B (280–315 nm), UV-A (315–400 nm) and PAR (400–700 nm).

2.3.2 Effective photochemical quantum yield

For the determination of the effective photochemical quantum yield (Φ_{PSII}), aliquots of 2 ml of sample from each tube (total of 9 tubes per CO₂ level, that is, triplicate per each radiation treatment) were taken every 1 min, both during exposure and recovery, and immediately measured (without any dark adaptation) using a xenon-pulse amplitude modulated fluorometer (XE-PAM, Walz, Germany). Each sample was measured 4 times and the Φ_{PSII} was determined by measuring the instant maximum fluorescence (F'_m) and the steady state fluorescence (F_t) of the light-adapted cells and calculated according to Genty et al. (1989) as: $\Phi_{\text{PSII}} = (F'_m - F_t)/F'_m = \Delta F/F'_m$. Non-photochemical quenching (NPQ) was calculated as: $\text{NPQ} = (F_m - F'_m)/F'_m$, where F_m represents the maximum fluorescence yield after dark adaptation for 10 min and F'_m the maximum fluorescence yield determined using a saturating white light pulse (5000 $\mu\text{mol photons m}^{-2} \text{s}^{-1}$ in 0.8 s) at the actinic light levels (300 $\mu\text{mol photons m}^{-2} \text{s}^{-1}$, similar to the exposure PAR level).

The inhibition of Φ_{PSII} due to UVR, UV-A, or UV-B was calculated as:

$$\text{Inh}_{\text{UVR}} (\%) = (\Phi_{\text{PSII P}} - \Phi_{\text{PSII PAB}})/(\Phi_{\text{PSII P}}) \times 100,$$

$$\text{Inh}_{\text{UV-A}} (\%) = (\Phi_{\text{PSII P}} - \Phi_{\text{PSII PA}})/(\Phi_{\text{PSII P}}) \times 100,$$

$$\begin{aligned} \text{Inh}_{\text{UV-B}} (\%) &= (\Phi_{\text{PSII PA}} - \Phi_{\text{PSII PAB}})/(\Phi_{\text{PSII P}}) \times 100 \\ &= \text{Inh}_{\text{UVR}} (\%) - \text{Inh}_{\text{UV-A}} (\%), \end{aligned}$$

where $\Phi_{\text{PSII P}}$, $\Phi_{\text{PSII PA}}$, and $\Phi_{\text{PSII PAB}}$ indicate the values of Φ_{PSII} in the P, PA and PAB treatments, respectively.

The rates of UV-induced damage to the photosynthetic apparatus (k , in min^{-1}) and repair (r , in min^{-1}) were estimated according to Heraud and Beardall (2000), applying the Kok model that assumes simultaneous operation of the damage and recovery during the photoinhibitory exposures, and calculated as follows: $Y = r/(r+k) + k/(r+k) * e^{-(r+k)*t}$, where Y represents Φ_{PSII} at t_n time.

2.3.3 Photosynthetic carbon uptake

Samples were inoculated with $5 \mu\text{Ci}$ (0.185 MBq) of labeled sodium bicarbonate (ICN Radiochemicals). A total of 20 tubes per CO_2 level (6 for each radiation treatment, plus 2 dark controls) were exposed under the solar simulator, with 3 tubes per radiation treatment (plus 2 dark) being filtered (Whatman GF/F, 25 mm) right after the 60 min of the exposures, while the other 9 tubes were filtered after the 60 min of recovery. After filtration, the filters were placed into 20 ml scintillation vials, exposed to HCl fumes overnight in darkness, and dried at 45°C for 4 h. Scintillation cocktail (Wallac Optiphase Hisafe 3, Perkin Elmer Life and Analytical Sciences, USA) was added to the vials, and the samples were counted after 1 h using a liquid scintillation counter (LS6500 Multi-Purpose Scintillation Counter, Beckman Counter, USA). The rate of photosynthetic carbon fixation was calculated according to Holm-Hansen and Helbling (1995). The inhibition due to UVR, UV-A or UV-B was determined in the same way as described for Φ_{PSII} .

2.3.4 Chlorophyll *a* (chl *a*)

Concentration of chl *a* at the beginning of the exposures was determined by filtering ~ 250 ml of culture onto a Whatman GF/F filter (diameter: 25 mm), extracted in 5 ml absolute methanol overnight at 4°C , and then centrifuged (10 min at 5000 g). The absorption spectrum of the supernatant was obtained by scanning the sample from 250 to 750 nm with a scanning spectrophotometer (DU 800, Beckman Coulter Inc) and the concentration of chl *a* was calculated using the equation of Porra (2002).

2.3.5 Data analysis

Three replicates for each radiation/temperature/ CO_2 condition were used in all experiments, so that the data is plotted as mean and standard deviation values. Three- and two-way ANOVA tests were used to determine the interaction between UVR, temperature and CO_2 concentration, or among two of these variables, respectively. The two-sample paired *t*-test was also used to determine significant differences between CO_2 , temperature or UV treatments. Significance level was set at $P < 0.05$.

3 Results

3.1 Carbonate system during semi-continuous growth

The pH levels in the LC or HC cultures were $8.16 (\pm 0.01)$ and $7.82 (\pm 0.02)$, respectively, being significantly different ($P < 0.01$, two-sample paired *t*-test). In the HC cultures, DIC, HCO_3^- and CO_2 levels were significantly higher by 11.8 %, 16.9 % and 156.3 %, respectively, and that of CO_3^{2-} was lower by 46.6 %. There was no significant difference in the total alkalinity between the two cultures, with the variations being < 0.4 %.

3.2 Growth and photochemical responses

The growth rate of the HC-grown *P. tricornutum* cells was higher by 3.7 % ($P = 0.001$) as compared to that of the LC-grown ones after being acclimated for more than 20 generations.

When exposed to UV radiation, the effective photochemical quantum yield (Φ_{PSII}) decreased significantly during the first 10–20 min of exposure in all radiation/temperature/ CO_2 treatments (Fig. 1); after this period, Φ_{PSII} remained more or less constant. These trends were best described and fitted using a first order exponential decrease function ($\Phi_{\text{PSII}} = a + b * e^{(-c*t)}$, where t represents the time of exposure, and a , b and c are adjustment parameters). Regardless of the temperature and CO_2 levels, the samples receiving PAR alone had less decrease in Φ_{PSII} (the lowest value reached ca. 0.5) after 10–20 min of exposure than those additionally receiving UV-A (in which Φ_{PSII} decreased to 0.3–0.4) or UV-A + B (Φ_{PSII} decreased to 0.2–0.3). At the same temperature level, HC-grown cells had generally better photochemical performance (i.e., higher Φ_{PSII}) than LC-grown ones, and this was more evident in the UV-treated samples. These differences in photochemical responses were clearly seen when plotting the Φ_{PSII} ratios of HC- to LC-grown cells (Fig. 2), which was ~ 1 in the P treatment at all temperatures. In the presence of UV-A or UV-A + UV-B, these trends were of increasing HC/LC Φ_{PSII} ratio during the 10–20 min of exposure, and then leveling off and maintaining rather constant values. The ratios HC/LC Φ_{PSII} , however, increased with increasing temperature: For example, under the PAB treatment, the ratios had mean values of 1.22, 1.30, and 1.41 for samples exposed at 15, 20 and 25°C , respectively. At 25°C , samples receiving UV-B had a significantly higher ($P < 0.01$) HC/LC Φ_{PSII} ratio than samples in the PA treatment; however, no significant differences were found between the PA and PAB treatments at 15 or 20°C ($P > 0.1$).

The rates of damage (k) and repair (r) during the exposures, estimated from the changes in Φ_{PSII} over time under different treatments, are presented in Fig. 3. There were differences in damage rates due to UV-A or UV-B (Fig. 3a and b) between the LC- and HC-grown cells, however changes were not significant at all temperature levels tested. In terms

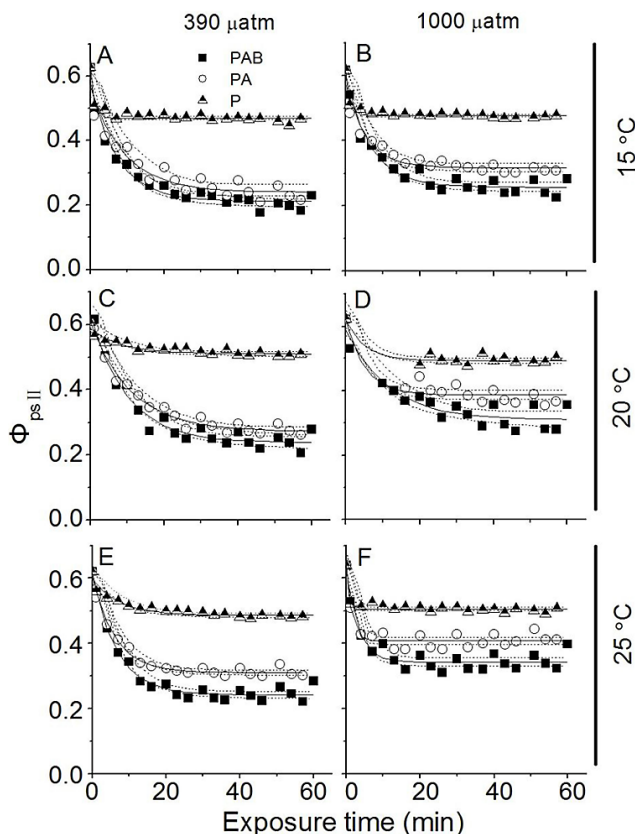


Fig. 1. Changes in effective photochemical quantum yield (Φ_{PSII}) of *P. tricornutum* cells grown under ambient (390 μatm , LC) (A, C and E) and elevated CO_2 (1000 μatm , HC) partial pressures (B, D and F) when exposed to solar radiation for 60 min under three radiation treatments – PAB (irradiated above 295 nm, black squares), PA (irradiances above 320 nm, white circles) and P (irradiances above 395 nm, half solid triangles) – at 15, 20 and 25 °C. Solid lines represent the best fit while the broken lines represent the 95 % confident limits.

of the effects caused by UV-A or UV-A + B (Fig. 3a and b), lower values were observed at 20 °C (growth temperature) in both LC- and HC-grown cells, although the difference was not significant either. The repair rates (Fig. 3c and d) in the presence of UV-A or UV-B appeared to be higher in the HC-grown cells, but the differences were also not significant.

In order to determine the potential “protecting” role of excess energy dissipation via non-photochemical quenching (NPQ), the variations of the ratio of repair (r) to damage (k), r/k , estimated from the changes in Φ_{PSII} over time were plotted against NPQ (Fig. 4). Inverse linear relationships were observed, with high r/k values associated with lower NPQ ones. Under the PA treatment, r/k in LC- and HC-grown cells had a similar decrease with increasing NPQ values (Fig. 4a). The addition of UV-B significantly reduced r/k ($P < 0.05$) (Fig. 4b) and led to a differential decrease of the ratio between the HC- and LC-grown cells. Nevertheless,

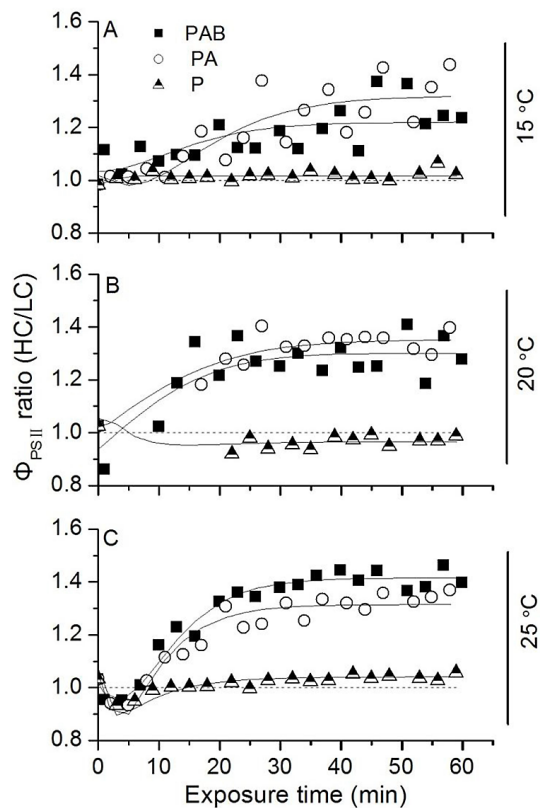


Fig. 2. Ratio of the HC- to LC-grown cells' effective quantum yield (Φ_{PSII}) in *P. tricornutum* exposed to the three radiation treatments – PAB (irradiated above 295 nm, black squares), PA (irradiances above 320 nm, white circles) and P (irradiances above 395 nm, half solid triangles) – at 15, 20 and 25 °C. Solid lines represent the best fit while the broken lines represent the value of 1.

HC-grown cells always had higher r/k than LC-grown cells at all NPQ values.

Once the stress was removed (i.e., after exposure, when the samples were shifted to low light levels), Φ_{PSII} recovered; this recovery was best described and fitted by a first order exponential equation: $\Phi_{PSII} = a + b \cdot (1 - e^{-c \cdot t})$, where t represents the time of exposure, and a , b and c are adjustment parameters (Fig. 5). Pre-exposure to UV-A and UV-B markedly hindered the recovery of Φ_{PSII} , especially in the 15 °C treatment for the LC-grown cells (Fig. 5a). However, the recovery rate of the LC-grown cells increased with temperature (Fig. 5a, c and e). In the HC-acclimated cells (Fig. 5b, d and f), the differences in recovery among the radiation treatments were not significant regardless of the preceding exposures to UV, with the exception of that incubated at 15 °C under the PAB treatment ($P < 0.05$). Within the same experimental temperature level, HC-grown cells had in general higher recovery rates than LC-grown ones, especially in cells that received UV.

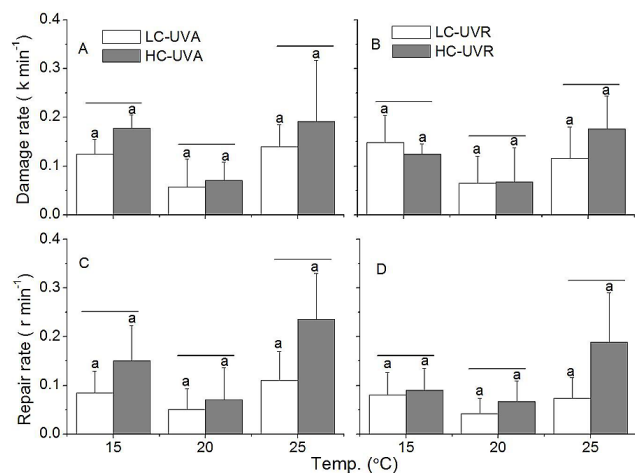


Fig. 3. Damage (k , in min^{-1}) and repair rates (r , in min^{-1}) of *P. tricornutum* cells grown at ambient (LC, white bars) and elevated CO_2 (HC, black bars) concentrations while exposed to radiation treatments with UV-A, (A) and (C), or UV-A + B, (B) and (D), at 15, 20 or 25 °C. The bars represent the means ($n = 3$) and the vertical lines are the standard deviation. Lines above histogram bars indicate significant difference between LC and HC, and the same letters indicate insignificant differences among the temperature treatments within the HC- or LC-grown cells.

3.3 Photosynthetic carbon fixation responses

Chl a content did not change throughout the exposure period within each CO_2 treatment, and there was no significant differences in the chl a content between the LC- and HC-grown cells (0.27 vs. 0.26 pg chl a cell $^{-1}$, $\text{SD} = 0.017$).

The photosynthetic carbon fixation rates during the exposures and recovery are shown in Fig. 6. After 60 min of exposure (Fig. 6a, c and e), the LC-grown cells had higher photosynthetic carbon fixation rates than the HC-grown ones, with the highest values found under the P treatment at 25 °C (~ 1.36 pg C cell $^{-1}$ h $^{-1}$). Moreover, the presence of UV-A or UV-A + UV-B reduced photosynthetic carbon fixation regardless of the growth CO_2 conditions or temperature levels. Increasing temperature from 15 °C (Fig. 6a) to 20 or 25 °C (Fig. 6c and e) significantly enhanced carbon fixation rates ($P < 0.01$). During the next 60 min recovery period, no significant differences among radiation treatments in the LC-grown cells were found at 15 or 25 °C (Fig. 6b and f), but at 20 °C carbon fixation was lower in the PAB than under the P or PA treatments (Fig. 6d). The HC-grown cells, instead, presented different responses: The lowest values were determined at 15 °C (Fig. 6b), whereas the highest were at 20 °C (Fig. 6d). When comparing photosynthetic carbon fixation rates among the exposure and recovery periods, it was seen that they were in general significantly higher ($P < 0.05$) when UV-A or UV-A + B was removed during the recovery period, except that at 25 °C. At 20 °C, the carbon fixation rate

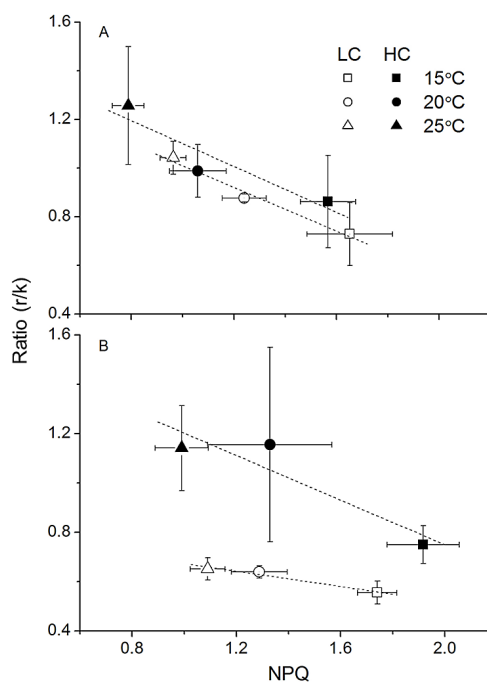


Fig. 4. Ratio of damage (k) to repair (r) as a function of non-photochemical quenching (NPQ) of *P. tricornutum* cells grown at ambient (LC, white symbols) and elevated CO_2 (HC, black symbols) concentrations when exposed to PAR + UV-A (A) or PAR + UV-A + UV-B (B) at 15 (squares), 20 (circles) or 25 °C (triangles). The broken lines represents linear regressions (A: $R^2 = 0.86$ (LC) and 0.98 (HC); B: $R^2 = 0.85$ (LC) and 0.97 (HC)).

was higher ($P < 0.01$) under the low PAR received during the recovery period, regardless the CO_2 levels.

When the UVR-induced inhibition of the photosynthetic carbon fixation was compared among the different CO_2 levels/temperatures (Fig. 7), it was seen that UV-A induced the highest inhibition at the lower temperature (15 °C) (Fig. 7a). The HC-grown cells showed higher sensitivity to UV-B at the lower temperature, but a reversed trend was observed at higher temperatures (20 and 25 °C), although the differences were not significant ($P > 0.1$). The “greenhouse” effects significantly reduced the photosynthetic inhibition ($P < 0.05$) caused by both UV-A (Fig. 7a) and UV-B (Fig. 7b).

4 Discussion

Global climate change brings about a combination of several factors that act together in such a way that they modify the dynamics of the ocean systems and hence, of the communities living there. In our study, we addressed the combined effects of three variables associated to climate change – ocean acidification (as addressed by a rise in CO_2 and H^+ concentrations), UV and temperature – on the cosmopolitan diatom *Phaeodactylum tricornutum*. Overall, we determined that the “greenhouse” treatment resulted in a generally better

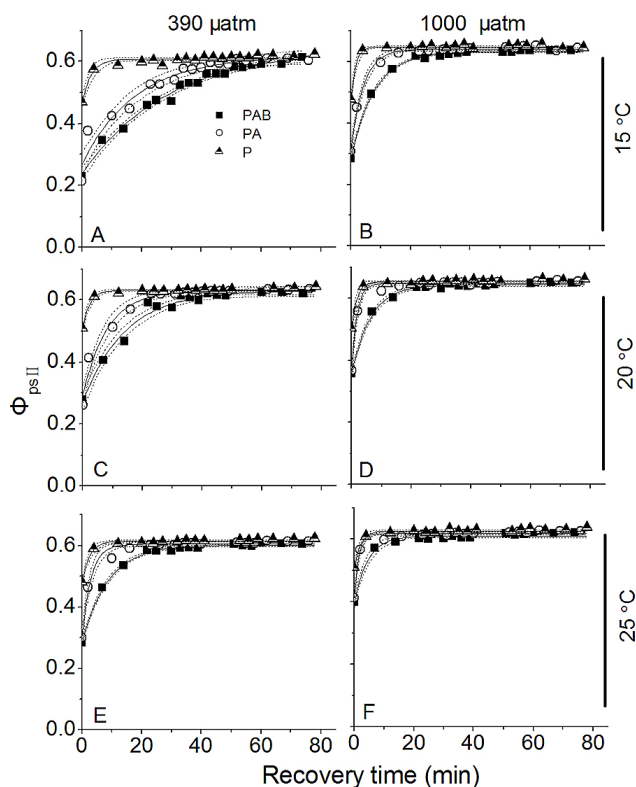


Fig. 5. Recovery of the effective photochemical quantum yield (Φ_{PSII}) in the LC- (A, C and E) and HC- (B, D and F) grown cells of *P. tricornutum* after exposure to three radiation treatments – PAB (irradiated above 295 nm, black squares), PA (irradiated above 320 nm, white circles) and P (irradiated above 395 nm, half solid triangles) – at 15, 20 and 25 °C. Solid lines represent the best fit while the broken lines represent the 95 % confident limits.

photosynthetic performance of this species and less sensitivity to UV.

In the present study we used the same strain of *P. tricornutum* as in previous studies carried out by Wu et al. (2010). Increased growth rate and unaffected cellular chl *a* content under the elevated CO_2 level were consistent between the present and those previous reports. Under the PAR alone treatment and increased temperature (Fig. 2b), the cells showed lower effective photosynthetic quantum yield under the elevated CO_2 levels, which also agrees with the previous findings by Wu et al. (2010), with HC-grown cells having higher inhibition of electron transport rate. However, when shifted to the lowest (15 °C) or highest (25 °C) temperature levels, this trend disappeared (Fig. 2a and c). However, Wu et al. (2010) reported that the NPQ for the HC-grown cells was lower than the LC ones when the cells grown at PAR intensities of $120 \mu\text{mol m}^{-2} \text{s}^{-1}$ were exposed to an actinic light of $840 \mu\text{mol m}^{-2} \text{s}^{-1}$ within a time frame < 5 min. In this work, HC-grown cells showed higher NPQ than the LC-grown ones, with exposures of about $300 \mu\text{mol m}^{-2} \text{s}^{-1}$ (PAR) for over 50 min and performing the determinations

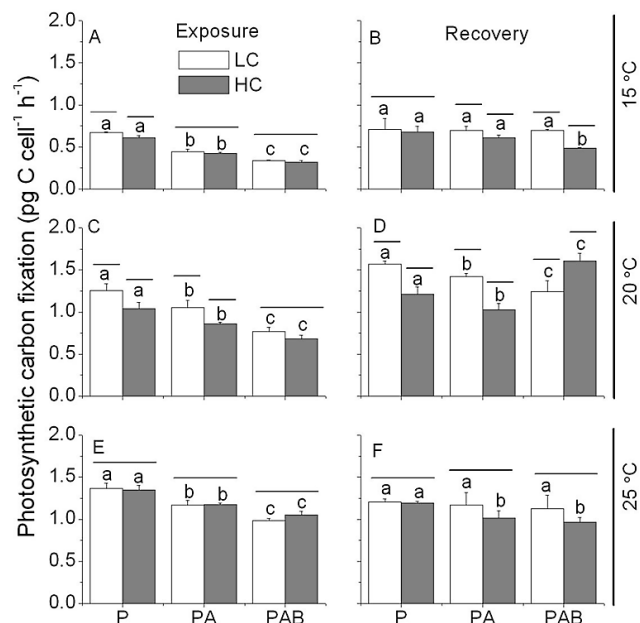


Fig. 6. Photosynthetic carbon fixation rates (in $\text{pg C cell}^{-1} \text{h}^{-1}$) in the LC- (white bars) and HC- (black bars) grown cells of *P. tricornutum* exposed to three radiation treatments – PAB (irradiated above 295 nm), PA (irradiated above 320 nm) and P (irradiated above 395 nm) – at 15, 20 and 25 °C. (A), (C) and (E) represent the carbon fixation rate during the 60 min exposure, while (B), (D) and (F) represent that during the 60 min recovery period. The bars represent the means ($n = 3$) and the vertical lines on top are the standard deviation. Lines above the histogram bars indicate significant differences between LC and HC, and different letters indicate significant differences among the radiation treatments within the HC- or LC-grown cells within each panel.

with the actinic light of $300 \mu\text{mol m}^{-2} \text{s}^{-1}$. The exposure time span might have accounted for part of this discrepancy in NPQ between this work and the previous study (Wu et al., 2010). In addition, since carbon concentration mechanisms (CCMs) of this diatom become down-regulated under elevated CO_2 (Burkhardt et al., 2001; Wu et al., 2010; Hopkinson et al., 2011), and levels of light can modulate the efficiency of CCMs (Bartual and Galvez, 2003; Raven, 2011; Reinfelder, 2011), the cells grown at 70 (present work) and $120 \mu\text{mol m}^{-2} \text{s}^{-1}$ (Wu et al., 2010) levels would have different levels of CCM operation efficiency or different levels of energetics; so that may be why the discrepancy might have occurred. In addition, NPQ under solar radiation (long exposures of about 12 h) was remarkably stimulated under elevated CO_2 levels of $1000 \mu\text{atm}$ (Gao et al., 2012).

When exposed to UV, the HC-grown cells had a better photochemical performance (i.e., smaller decrease of Φ_{PSII}) than those grown in LC conditions, with the ratio of Φ_{PSII} in HC- to that in the LC-grown cells > 1 (Fig. 2), indicating that UV and high CO_2 synergistically raised the yield. When the UV-induced inhibition of photosynthetic carbon

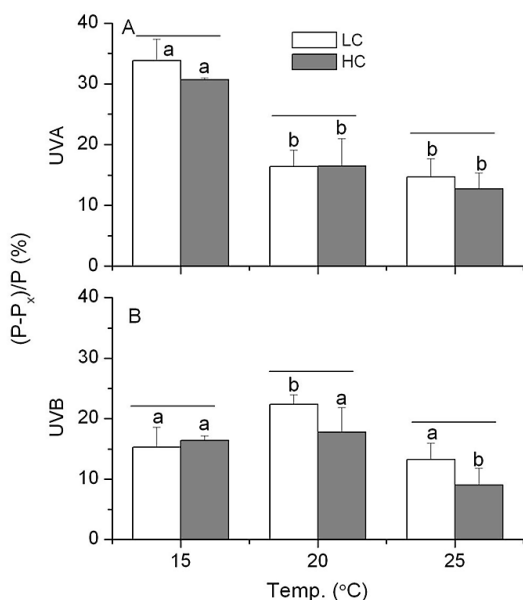


Fig. 7. Inhibition of photosynthetic carbon fixation of *P. tricornutum* grown at ambient (LC, white bars) and elevated CO₂ (HC, black bars) concentrations due to UV-A (A) or UV-B (B) exposed to three radiation treatments for 60 min at 15, 20 and 25 °C. The bars represent the means ($n = 3$), and the vertical lines on top are the standard deviation. Lines above the histogram bars indicate significant difference between LC and HC, and different letters indicate significant differences among the temperature treatments within the HC- or LC-grown cells.

fixation was examined (Fig. 7), obviously, the high CO₂ level acted to reduce the UV-B-induced inhibition of photosynthesis, though the absolute photosynthetic carbon fixation rates were higher under the PAR-alone treatments compared to those with UV (Fig. 6). It has been previously found that effects of climate change variables (temperature and UV) were different according to the photosynthetic targets examined (Helbling et al., 2011), which could explain at least part of the differences observed between LC and HC pre-acclimated cells. Moreover, Wu et al. (2010) found for *P. tricornutum* that respiration was enhanced in the HC-grown cells and that its carbon concentration mechanisms (CCMs) were down-regulated. Photorespiration was also higher in the HC-grown cells of this species (Gao et al., 2012). On the other hand, high contribution of net CO₂ uptake (about two-thirds) to total inorganic carbon acquisition was reported in *P. tricornutum* (Burkhardt et al., 2001; Hopkinson et al., 2011). Together with the down-regulation of CCM (meaning a lowered active uptake of inorganic carbon), enhancement of mitochondrial- and photo-respiration could have led to decreased photosynthetic carbon fixation due to the additional carbon losses. The stimulated quantum yield in the HC-grown cells appeared to be attributed to the extra carbon loss, i.e., extra electron drainage due to enhanced photorespiration, which provided a protective role.

The UV-induced inhibition of the effective photochemical quantum yield was inversely correlated with temperature. The ratios of repair to damage (r/k) decreased with increasing NPQ (Fig. 4). Similarly, in the diatoms *Thalassiosira pseudonana* and *Coscinodiscus radiates*, when repair and photoinactivation are balanced, NPQ induction is small. NPQ induction increased under treatment conditions where photoinactivation exceeded repair (Wu et al., 2012). At the low temperature, the LC-grown cells showed higher UV-induced inhibition of photochemical efficiency (Fig. 1), and the recovery was slower (Fig. 5) compared with the HC-grown ones. The “greenhouse” treatment resulted in a significant ($P < 0.05$) decrease of UV-induced inhibition from 50–60% to 27–36%, of which UV-B accounted for about 8% and 14%, respectively. This trend appears to be similar to the changes observed in photosynthetic carbon fixation, as increase in its rates with increasing temperature was higher in the HC- than in the LC-grown cells (Fig. 6a, c and e), reflecting a synergistic effect of $p\text{CO}_2$ rise and warming. This might be associated with enhanced activity of cellular enzymes and membrane fluidity, as they are temperature-dependent (Allakhverdiev et al., 2008), and accelerated molecular repair rates that usually increase with temperature within a species’ thermal window (Conkling and Drake, 1984; Gao et al., 2008). In the presence of UV-B, NPQ in the LC-grown cells was lower than HC-grown ones, especially under the lower temperature treatment (Fig. 4b). Down-regulation of CCM might have aided to enhance NPQ in the HC-grown cells due to the saved energy demand for CO₂ active uptake, which could lead to an additional light stress (Gao et al., 2012). Activity and gene expression of Rubisco in the diatom *Thalassiosira weissflogii* increased with increased temperature, and this might have partially counteracted the UV-induced inhibition of photosynthetic carbon fixation (Helbling et al., 2011). On the other hand, high levels of UV can lead to degradation of periplasmic carbonic anhydrase (CAe) (Wu and Gao, 2009), as well as Rubisco and D1 protein (Bischof et al., 2002; Bouchard et al., 2005), and increased temperature could have stimulated the repair of the damaged molecules. The beneficial effects of increased temperature on photosynthesis under UV stress have been previously documented (Sobrino and Neale, 2007; Gao et al., 2008; Halac et al., 2010; Helbling et al., 2011), showing lower UV-induced inhibition or damages at higher temperatures. Differential sensitivities to UV have been reported in marine picoplankters when grown under elevated CO₂ concentrations, with *Nannochloropsis gaditana* having lower sensitivity while *Nannochloris atomus* showed neutral response (Sobrino et al., 2005). For the diatom *Thalassiosira pseudonana*, when grown at elevated CO₂ concentration, it became more sensitive to UV (Sobrino et al., 2008). In the present study, when the photosynthetic carbon fixation and Φ_{PSII} were compared, the UV-induced inhibition was lower on the former than on the latter, and higher CO₂ weakened this inhibition. Regardless of the pre-acclimation CO₂ levels,

less inhibition caused by UV on carbon fixation might be due to stimulation of the activity of CAe (Wu and Gao, 2009), which catalyzes the inter-conversion of bicarbonate and CO₂, therefore stimulating the uptake of CO₂ during the exposures. Additionally, the increase of r/k with temperature was higher in the HC- than in the LC-grown cells, which reflects enhanced repair in these cells, as UV-induced molecular damage was independent of temperature (Ishigaki et al., 1999).

In terms of ecological implications, future “greenhouse” ocean with decreased thickness of the upper mixing layer (enhanced stratification) may expose phytoplankton cells to higher exposures of solar UV as well as PAR. For diatoms like *P. tricornutum*, increased CO₂ and seawater acidity might counteract somehow the harm caused by UV-B. Since UV-A results in negative effects on phytoplankton carbon fixation under high solar radiation but positive ones under reduced levels of solar radiation, playing a double-edged effect on phytoplankton (Gao et al., 2007b), its stimulating effects would be enlarged under ocean acidification conditions (Chen and Gao, 2011). Thus, the net effects of UV, temperature and CO₂ will largely depend on the levels of solar radiation to which the phytoplankton cells are exposed. Consequently, mixing rates or mixing depth will explicitly affect the combined effects of the above climate change variables, as mixing exposes cells to fluctuating irradiances which can affect the balance between photodamage and repair of PS II. Increased NPQ, as found in this study, closely related to the decreases (UV-related) of the ratio between repair and damage rate (r/k) of PS II in *P. tricornutum*. The increased seawater acidity must have stimulated photoprotective processes, thus, leading to higher NPQ, which was especially pronounced in the presence of UV-B (Fig. 4). Increasing temperature, in some cold or temperate waters, may help the species like *P. tricornutum* to counteract negative effects of UVR or ocean acidification-induced harm. On the other hand, variable responses to combined effects of climate change variables are expected in view of their diversities in physiological pathways and ecological niches.

Acknowledgements. This study was supported by National Basic Research Program of China (No. 2009CB421207 and 2011CB200902), Program for Changjiang Scholars and Innovative Research Team (IRT0941), National Natural Science Foundation (No. 40930846, No. 41120164007) and China-Japan collaboration project from MOST (S2012GR0290), and Consejo Nacional de Investigaciones Científicas y Técnicas –Argentina (PIP 12-201001-00228). VEV and EWH were supported by the Visiting Professor Program (111) from the Ministry of Education of China. We thank the comments of D. Campbell and of two anonymous reviewers that helped to improve this manuscript. This is Contribution No. 127 of Estación de Fotobiología Playa Unión.

Edited by: E. Marañón

References

- Alexiadis, A.: Global warming and human activity: A model for studying the potential instability of the carbon dioxide/temperature feedback mechanism, *Ecol. Model.*, 203, 243–256, doi:10.1016/j.ecolmodel.2006.11.020, 2007.
- Allakhverdiev, S., Kreslavski, V. D., Klimov, V. V., Los, D. A., Carpentier, R., and Mohanty, P.: Heat stress: an overview of molecular responses in photosynthesis, *Photosynth. Res.*, 98, 541–550, doi:10.1007/s11120-008-9331-0, 2008.
- Barbieri, E. S., Villafañe, V. E., and Helbling, E. W.: Experimental assessment of UV effects on temperate marine phytoplankton when exposed to variable radiation regimes, *Limnol. Oceanogr.*, 47, 1648–1655, 2002.
- Bartual, A. and Galvez, J. A.: Short- and long-term effects of irradiance and CO₂ availability on carbon fixation by two marine diatoms, *Can. J. Bot.*, 81, 191–200, 2003.
- Beaufort, L., Probert, I., de Garidel-Thoron, T., Bendif, E. M., Ruiz-Pino, D., Metzl, N., Goyet, C., Buchet, N., Coupel, P., Grelaud, M., Rost, B., Rickaby, R. E. M., and de Vargas, C.: Sensitivity of coccolithophores to carbonate chemistry and ocean acidification, *Nature*, 476, 80–83, doi:10.1038/nature10295, 2011.
- Beardall, J., Sobrino, C., and Stojkovic, S.: Interactions between the impacts of ultraviolet radiation, elevated CO₂, and nutrient limitation on marine primary producers, *Photochem. Photob. S.*, 8, 1257–1265, doi:10.1039/b9pp00034h, 2009.
- Bischof, K., Kräbs, G., Wiencke, C., and Hanelt, D.: Solar ultraviolet radiation affects the activity of ribulose-1, 5-bisphosphate carboxylase-oxygenase and the composition of photosynthetic and xanthophyll cycle pigments in the intertidal green alga *Ulva lactuca* L., *Planta*, 215, 502–509, doi:10.1007/s00425-002-0774-9, 2002.
- Bouchard, J. N., Campbell, D. A., and Roy, S.: Effects of UV-B radiation on the D1 protein repair cycle of natural phytoplankton communities from three latitudes (Canada, Brazil, and Argentina), *J. Phycol.*, 41, 273–286, 2005.
- Boyd, P. W.: Beyond ocean acidification, *Nat. Geosci.*, 4, 273–274, doi:10.1038/ngeo1150, 2011.
- Burkhardt, S., Amoroso, G., Riebesell, U., and Sültermeyer, D.: CO₂ and HCO₃⁻ uptake in marine diatoms acclimated to different CO₂ concentrations, *Limnol. Oceanogr.*, 46, 1378–1391, 2001.
- Cai, W.-J., Hu, X. P., Huang, W.-J., Murrell, M. C., Lehrter, J. C., Lohrenz, S. E., Chou, W.-C., Zhai, W. D., Hollibaugh, J. T., Wang, Y. C., Zhao, P. S., Guo, X. H., Gundersen, K., Dai, M. H., and Gong, G.-C.: Acidification of subsurface coastal waters enhanced by eutrophication, *Nat. Geosci.*, 4, 766–770, doi:10.1038/NGEO1297, 2011.
- Caldeira, K. and Wickett, M. E.: Anthropogenic carbon and ocean pH, *Nature*, 425, 365, doi:10.1038/425365a, 2003.
- Chen, S. W. and Gao, K. S.: Solar ultraviolet radiation and CO₂-induced ocean acidification interacts to influence the photosynthetic performance of the red tide alga *Phaeocystis globosa* (Prymnesiophyceae), *Hydrobiologia*, 675, 105–117, doi:10.1007/s10750-011-0807-0, 2011.
- Christensen, M. R., Graham, M. D., Vinebrooke, R. D., Findlay, D. L., Paterson, M. J., and Turner, M. A.: Multiple anthropogenic stressors cause ecological surprises in boreal lakes, *Global Change Biol.*, 12, 2316–2322, doi:10.1111/j.1365-2486.2006.01257.x, 2006.

- Cloern, J. E., Schraga, T. S., Lopez, C. B., Knowles, N., Labisoa, R. G., and Dugdale, R.: Climate anomalies generate an exceptional dinoflagellate bloom in San Francisco Bay, *Geophys. Res. Lett.*, 32, L14608, doi:10.1029/2005GL023321, 2005.
- Conkling, M. A. and Drake, J. W.: Thermal rescue of UV-irradiated bacteriophage T4 and biphasic mode of action of the WXY system, *Genetics*, 107, 525–536, 1984.
- Dickson, A. G.: Standard potential of the reaction: $\text{AgCl(s)} + 1/2 \text{H}_2(\text{g}) = \text{Ag(s)} + \text{HCl(aq)}$, and the standard acidity constant of the ion HSO_4^- in synthetic seawater from 273.15 to 318.15 K, *J. Chem. Thermodyn.*, 22, 113–127, 1990.
- Doney, S. C.: The dangers of ocean acidification, *Sci. Amer.*, 294, 58–65, 2006.
- Dunne, R. P.: Synergy or antagonism – interactions between stressors on coral reefs, *Coral Reefs*, 29, 145–152, doi:10.1007/s00338-009-0569-6, 2010.
- Feng, Y. Y., Hare, C. E., Leblanc, K., Rose, J. M., Zhang Y. H., DiTullio, G. R., Lee, P. A., Wilhelm, S. W., Rowe, J. M., Sun, J., Nemcek, N., Gueguen, C., Passow, U., Benner, I., Brown, C., and Hutchins, D. A.: Effects of increased $p\text{CO}_2$ and temperature on the North Atlantic spring bloom, I. The phytoplankton community and biogeochemical response, *Mar. Ecol.-Prog. Ser.*, 388, 13–25, doi:10.3354/meps08133, 2009.
- Figueroa, F. L., Salles, S., Aguilera, J., Jiménez, C., Mercado, J., Viinegla, B., FloresMoya, A., and Altamirano, M.: Effects of solar radiation on photoinhibition and pigmentation in the red *Porphyra leucosticta*, *Mar. Ecol.-Prog. Ser.*, 151, 81–90, 1997.
- Fu, F. X., Mark, E. W., Zhang Y. H., Feng Y. Y., and Hutchins, D. A.: Effects of increased temperature and CO_2 on photosynthesis, growth, and elemental ratios in marine *Synechococcus* and *Prochlorococcus* (Cyanobacteria), *J. Phycol.*, 43, 485–496, doi:10.1111/j.1529-8817.2007.00355.x, 2007.
- Fu, F. X., Zhang, Y. H., Warner, M. E., Feng, Y. Y., and Hutchins, D. A.: A comparison of future increased CO_2 and temperature effects on sympatric *Heterosigma akashiwo* and *Prorocentrum minimum*, *Harmful Algae*, 7, 76–90, doi:10.1016/j.hal.2007.05.006, 2008.
- Gao, K. S. and Zheng, Y. Q.: Combined effects of ocean acidification and solar UV radiation on photosynthesis, growth, pigmentation and calcification of the coralline alga *Corallina sessilis* (Rhodophyta), *Global Change Biol.*, 16, 2388–2398, doi:10.1111/j.1365-2486.2009.02113.x, 2010.
- Gao, K. S., Aruga, Y., Asada, K., Ishihara, T., Akano, T., and Kiyohara, M.: Calcification in the articulated coralline algal *Corallina pilulifera*, with special reference to the effect of elevated CO_2 concentration, *Mar. Biol.*, 117, 129–132, 1993.
- Gao, K. S., Guan, W. C., and Helbling, E. W.: Effects of solar ultraviolet radiation on photosynthesis of the marine red tide alga *Heterosigma akashiwo* (Raphidophyceae), *J. Photoch. Photobio. B*, 86, 140–148, doi:10.1016/j.jphotobiol.2006.05.007, 2007a.
- Gao, K. S., Wu, Y. P., Li, G., Wu, H. Y., Villafañe, V. E., and Helbling, E. W.: Solar UV radiation drives CO_2 fixation in marine phytoplankton: A double-edged sword, *Plant Physiol.*, 144, 54–59, doi:10.1104/pp.107.098491, 2007b.
- Gao, K. S., Li, P., Walanabe, T., and Helbling, E. W.: Combined effects of ultraviolet radiation and temperature on morphology, photosynthesis, and DNA of *Arthrospira (Spirulina) platensis* (Cyanophyta), *J. Phycol.*, 44, 777–786, doi:10.1111/j.1529-8817.2008.00512.x, 2008.
- Gao, K. S., Ruan, Z. X., Villafañe, V. E., Gattuso, J.-P., and Helbling, E. W.: Ocean acidification exacerbates the effect of UV radiation on the calcifying phytoplankter *Emiliania huxleyi*, *Limnol. Oceanogr.*, 54, 1855–1862, 2009.
- Gao, K. S., Xu, J. T., Gao, G., Li, Y. H., Hutchins, D. A., Huang, B. Q., Wang, L., Zheng, Y., Jin, P., Cai, X. N., Häder, D.-P., Li, W., Xu, K., Liu, N. N., and Riebesell, U.: Rising CO_2 and increased light exposure synergistically reduce marine primary productivity, *Nat. Clim. Change*, 2, 519–523, doi:10.1038/NCLIMATE1507, 2012.
- Genty, B. E., Briantais, J. M., and Baker, N. R.: Relative quantum efficiencies of the two photosystems of leaves in photorespiratory and non-photorespiratory conditions, *Plant Physiol. Biochem.*, 28, 1–10, 1989.
- Grzymiski, J., Orrico, C., and Schofield, O. M.: Monochromatic ultraviolet light induced damage to Photosystem II efficiency and carbon fixation in the marine diatom *Thalassiosira pseudonana* (3H), *Photosynth. Res.*, 68, 181–192, 2001.
- Guan, W. C. and Gao, K. S.: Impacts of UV radiation on photosynthesis and growth of coccolithophore *Emiliania huxleyi* (Haptophyceae), *Environ. Exp. Bot.*, 67, 502–508, doi:10.1016/j.envexpbot.2009.08.003, 2010.
- Halac, S. R., Villafañe, V. E., and Helbling, E. W.: Temperature benefits the photosynthetic performance of the diatoms *Chaetoceros gracilis* and *Thalassiosira weissflogii* when exposed to UVR, *J. Photoch. Photobio. B.*, 101, 196–205, doi:10.1016/j.jphotobiol.2010.07.003, 2010.
- Hallegraeff, G. M.: Ocean climate change, phytoplankton community responses, and harmful algal blooms: a formidable predictive challenge, *J. Phycol.*, 46, 220–235, doi:10.1111/j.1529-8817.2010.00815.x, 2010.
- Hare, C. E., Leblanc, K., DiTullio, G. R., Kudela, R. M., Zhang, Y. H., Lee, P. A., Riseman, S., and Hutchins, D. A.: Consequences of increased temperature and CO_2 for phytoplankton community structure in the Bering Sea, *Mar. Ecol.-Prog. Ser.*, 352, 9–16, doi:10.3354/meps07182, 2007.
- Hein, M. and Sand-Jensen, K.: CO_2 increases oceanic primary production, *Nature*, 388, 526–527, 1997.
- Helbling, E. W., Villafañe, V. E., Ferrario, M. E., and Holm-Hansen, O.: Impact of natural ultraviolet radiation on rates of photosynthesis and on specific marine phytoplankton species, *Mar. Ecol.-Prog. Ser.*, 80, 89–100, 1992.
- Helbling, E. W., Buma, A. G. J., Boelen, P., van der Strate, H. J., Fiorda Giordanino, M. V., and Villafañe, V. E.: Increase in Rubisco activity and gene expression due to elevated temperature partially counteracts ultraviolet radiation-induced photoinhibition in the marine diatom *Thalassiosira weissflogii*, *Limnol. Oceanogr.*, 56, 1330–1342, doi:10.4319/lo.2011.56.4.1330, 2011.
- Heraud, P. and Beardall, J.: Changes in chlorophyll fluorescence during exposure of *Dunaliella tertiolecta* to UV radiation indicate a dynamic interaction between damage and repair processes, *Photosynth. Res.*, 63, 123–134, 2000.
- Holm-Hansen, O. and Helbling, E. W.: Técnicas para la medición de la productividad primaria en el fitoplancton, in: *Manual de Métodos Ficológicos*, edited by: Alveal, K., Ferrario, M. E., Oliveira, E. C., and Sar, E., Universidad de Concepción, Concepción, Chile, 329–350, 1995.

- Hopkinson, B. M., Dupont, C. L., Allen, A. E., and Morel, F. M. M.: Efficiency of the CO₂-concentrating mechanism of diatom, *P. Natl. Acad. Sci. USA*, 108, 3830–3837, doi:10.1073/pnas.1018062108, 2011.
- Houghton, J. T., Ding, Y., Griggs, D. J., Noguer, M., Van Der Linden, P. J., Dai, X., Mashell, L., and Johnson, C. A.: Climate change 2001: the scientific basis, Cambridge University Press, Cambridge, 2001.
- Hutchins, D. A.: Oceanography: Forecasting the rain ratio, *Nature*, 476, 41–42, doi:10.1038/476041a, 2011.
- Hutchins, D. A., Fu, F. X., Zhang, Y. H., Warner, M. E., Feng, Y. Y., Portune, K., Bernhardt, P. W., and Mulholland, M. R.: CO₂ control of *Trichodesmium* N₂ fixation, photosynthesis, growth rates, and elemental ratios: Implications for past, present, and future ocean biogeochemistry, *Limnol. Oceanogr.*, 52, 1293–1304, 2007.
- Ishigaki, Y., Takayama, A., Yamashita, S., and Nikaido, O.: Development and characterization of a DNA solar dosimeter, *J. Photoch. Photobio. B*, 50, 184–188, 1999.
- Jiang, H. B. and Qiu, B. S.: Inhibition of photosynthesis by UV-B exposure and its repair in the bloom-forming cyanobacterium *Microcystis aeruginosa*, *J. Appl. Phycol.*, 23, 691–696, doi:10.1007/s10811-010-9562-2, 2011.
- Lewandowska, A. and Sommer, U.: Climate change and the spring bloom: a mesocosm study on the influence of light and temperature on phytoplankton and mesozooplankton, *Mar. Ecol.-Prog. Ser.*, 405, 101–111, doi:10.3354/meps08520, 2010.
- Lewis, E. and Wallace, D. W. R.: Program Developed for CO₂ System Calculations, ORNL/CDIAC-105, Carbon Dioxide Information Analysis Center, Oak Ridge National Laboratory, US Department of Energy, 1998.
- Manney, G. L., Santee, M. L., Rex, M., Livesey, N. J., Pitts, M. C., Veefkind, P., Nash, E. R., Wohltmann, I., Lehmann, R., Froidevaux, L., Poole, L. R., Schoeberl, M. R., Haffner, D. P., Davies, J., Dorokhov, V., Gernandt, H., Johnson, B., Kivi, R., Kyrö, E., Larsen, N., Levelt, P. F., Makshtas, A., McElroy, T., Nakajima, H., Parrondo, M. C., Tarasick, D. W., von der Gathen, P., Walker, K. A., and Zinoviev, N. S.: Unprecedented Arctic ozone loss in 2011, *Nature*, 478, 469–475, doi:10.1038/nature10556, 2011.
- McCarthy, A., Rogers, S. P., Duffy, S. J., and Campbell, D. A.: Elevated carbon dioxide differentially alters the photo-physiology of *Thalassiosira pseudonana* (Bacillariophyceae) and *Emiliania huxleyi* (Haptophyta), *J. Phycol.*, 47, 635–646, doi:10.1111/j.1529-8817.2012.01171.x, 2012.
- McNeil, B. I. and Matear, R. J.: Southern Ocean acidification: A tipping point at 450-ppm atmospheric CO₂, *P. Natl. Acad. Sci. USA*, 105, 18860–18864, 2008.
- Merico, A., Tyrrell, T., Lessard, E. J., Oguz, T., Stabeno, P. J., Zeeman, S. I., and Whitledge, T. E.: Modelling phytoplankton succession on the Bering Sea shelf: role of climate influences and trophic interactions in generating *Emiliania huxleyi* blooms 1997–2000, *Deep-Sea Res.*, 51, 1803–1826, doi:10.1016/j.dsr.2004.07.003, 2004.
- Morel, F. M. M., Rueter, J. G., Anderson, D. M., and Guillard, R. R. L.: Aquil: A chemically defined phytoplankton culture medium for trace metal studies, *J. Phycol.*, 15, 135–141, 1979.
- Mühling, M., Harris, N., Belay, A. and Whitton, B. A.: Reversal of helix orientation in the cyanobacterium *Arthrospira*, *J. Phycol.*, 39, 360–367, 2003.
- Mühling, M., Belay, A., and Whitton, B. A.: Variation in fatty acid composition of *Arthrospira* (Spirulina) strains, *J. Appl. Phycol.*, 17, 137–146, doi:10.1007/s10811-005-7213-9, 2005.
- Nilawati, J., Greenberg, B. M., and Smith, R. E. H.: Influence of ultraviolet radiation on growth and photosynthesis of two cold ocean diatoms, *J. Phycol.*, 33, 215–224, 1997.
- Orr, J. C., Fabry, V. J., Aumont, O., Bopp, L., Doney, S. C., Feely, R. A., Gnanadesikan, A., Gruber, N., Ishida, A., Joos, F., Key, R. M., Lindsay, K., Maier-Reimer, E., Matear, R., Monfray, P., Mouchet, A., Najjar, R. G., Plattner, G. K., Rodgers, K. B., Sabine, C. L., Sarmiento, J. L., Schlitzer, R., Slater, R. D., Totterdell, I. J., Weirig, M. F., Yamanaka, Y., and Yool, A.: Anthropogenic ocean acidification over the twenty-first century and its impact on calcifying organisms, *Nature*, 437, 681–686, 2005.
- Peperzak, L.: Climate change and harmful algal blooms in the North Sea, *Acta Oecol.*, 24, S139–S144, 2003.
- Porra, R. J.: The chequered history of the development and use of simultaneous equations for the accurate determination of chlorophylls *a* and *b*, *Photosynth. Res.*, 73, 149–156, 2002.
- Raven, J. A., Giordano, M., Beardall, J., and Maberly, S. C.: Algal and aquatic plant carbon concentrating mechanisms in relation to environmental change, *Photosynth. Res.*, 109, 281–296, doi:10.1007/s11120-011-9632-6, 2011.
- Reinfelder, J. R.: Carbon concentrating mechanisms in eukaryotic marine phytoplankton, *Annu. Rev. Mar. Sci.*, 3, 291–315, doi:10.1146/annurev-marine-120709-142720, 2011.
- Riebesell, U. and Tortell, P. D.: Effects of ocean acidification on pelagic organisms and ecosystems, in: Ocean acidification, edited by: Gattuso, J.-P. and Hansson, L., Oxford University Press, UK, 99–116, 2011.
- Riebesell, U., Schulz, K. G., Bellerby, R. G. J., and Botros, M.: Enhanced biological carbon consumption in a high CO₂ ocean, *Nature*, 450, 545–548, doi:10.1038/nature06267, 2007.
- Roy, R. N., Roy, L. N., Vogel, K. M., Porter-Moore, C., Pearson, T., Good, C. E., Millero, F. J., and Campbell, D. M.: The dissociation constants of carbonic acid in seawater at salinities 5 to 45 and temperature 0 to 45 °C, *Mar. Chem.*, 44, 249–267, 1993.
- Sabine, L. C., Feely, R. A., Gruber, N., Key, R. M., Lee, K., Bullister, J. L., Wanninkhof, R., Wong, C. S., Wallace, D. W. R., Tilbrook, B., Millero, F. J., Peng, T.-H., Kozyr, A., Tsuno, O., and Rios, A. F.: The oceanic sink for anthropogenic CO₂, *Science*, 305, 367–371, doi:10.1126/science.1097403, 2004.
- Schippers, P., Lurling, M., and Scheffer, M.: Increase of atmospheric CO₂ promotes phytoplankton productivity, *Ecol. Lett.*, 7, 446–451, doi:10.1111/j.1461-0248.2004.00597.x, 2004.
- Sobrinho, C. and Neale, P. J.: Short-term and long-term effects of temperature on photosynthesis in the diatom *Thalassiosira pseudonana* under UVR exposures, *J. Phycol.*, 43, 426–436, doi:10.1111/j.1529-8817.2007.00344.x, 2007.
- Sobrinho, C., Neale, P. J., and Lubian, L. M.: Interaction of UV radiation and inorganic carbon supply in the inhibition of photosynthesis: Spectral and temporal responses of two marine picoplankters, *Photochem. Photob.*, 81, 384–393, 2005.
- Sobrinho, C., Ward, M. L., and Neale, P. J.: Acclimation to elevated carbon dioxide and ultraviolet radiation in the diatom *Thalassiosira pseudonana*: Effects on growth, photosynthesis, and spectral sensitivity of photoinhibition, *Limnol. Oceanogr.*, 53, 494–505, 2008.

- Tortell, P. D. and Morel, M. M.: Sources of inorganic carbon for phytoplankton in the Eastern Subtropical and Equatorial Pacific Ocean, *Limnol. Oceanogr.*, 47, 1012–1022, 2002.
- Tortell, P. D., Rau, G. H., and Morel, F. M. M.: Inorganic carbon acquisition in coastal Pacific phytoplankton communities, *Limnol. Oceanogr.*, 45, 1485–1500, 2000.
- Tortell, P. D., Ditullio, G. R., Sigmann, D. M., and Morel, F. M. M.: CO₂ effects on taxonomic composition and nutrient utilization in an Equatorial Pacific phytoplankton assemblage, *Mar. Ecol.-Prog. Ser.*, 236, 37–43, 2002.
- Wu, H. Y. and Gao, K. S.: Ultraviolet radiation stimulated activity of extracellular carbonic anhydrase in the marine diatom *Skeletonema costatum*, *Funct. Plant Biol.*, 36, 137–143, 2009.
- Wu, Y., Gao, K., and Riebesell, U.: CO₂-induced seawater acidification affects physiological performance of the marine diatom *Phaeodactylum tricorutum*, *Biogeosciences*, 7, 2915–2923, doi:10.5194/bg-7-2915-2010, 2010.
- Wu, H. Y., Roy, S., Alami, M., Green, B. R., and Campbell, D. A.: Photosystem II photoinactivation, repair and protection in marine centric diatoms, *Plant Physiol.*, 160, 464–476, doi:10.1104/pp.112.203067, 2012.
- Xiong, F. S.: Evidence that UV-B tolerance of the photosynthetic apparatus in microalgae is related to the D1-turnover mediated repair cycle in vivo, *J. Plant Physiol.*, 158, 285–294, 2001.
- Xu, K., Gao, K., Villafañe, V. E., and Helbling, E. W.: Photosynthetic responses of *Emiliania huxleyi* to UV radiation and elevated temperature: roles of calcified coccoliths, *Biogeosciences*, 8, 1441–1452, doi:10.5194/bg-8-1441-2011, 2011.